V FROG (Foam, Rain, Oil Slicks and GPS reflections) experiment plan

V.1 Introduction and scientific objectives

The main goal of the WISE field experiments consisted of improving the sea surface emissivity models by taking L-band radiometric measurements of the sea surface, and studying specifically the deviations from the flat surface model due to sea state and sea foam. According to the results of the WISE experiments, the impact of foam in the brightness temperatures is clear above 12 m/s wind speed, although it is difficult to determine it, since many other parameters (wind speed, atmospheric stability, swell, and the finite radiometric sensitivity) intervene in the emissivity variations measured by the radiometer. Hence, to minimize the high variability of the emissivity, a specific campaign (FROG) was performed during the spring of 2003. The main objectives of the FROG 2003 field experiment were fourfold:

- Acquisition of radiometric measurements of an artificially generated foam-covered water surface,
- Acquisition of foam vertical profile snapshots, and measurement of the main parameters such as: foam thickness, radii bubbles histogram, air-water content vs. depth, bubble's water coating thickness, and the stickyness factor. These parameters will be later used as the inputs of the two-layer foam emission model to make an inter-comparison between its output and the measured foam emissivity,
- Acquisition of radiometric measurements of an artificially-generated rain, and
- Acquisition of radiometric measurements of a water surface covered by oil slicks.

V.2 Experiment description

V.2.1 Experimental set-up

To achieve the goals of FROG field experiments, it was necessary to build

- a foam generator, and
- a rain generator.

To minimize the radiation collected from buildings etc., and reflect the sky radiation, thus enlarging the radio-electric horizon, the pool was surrounded by a metallic net, which in its upper part was inclined 45° with respect to the horizon.

In addition, it was necessary to analyze the water samples acquired at each sequence (ICM), in order to accurately determine its salinity.

V.2.1.1 Foam generator

An array of 104 air diffusers was mounted in the pool floor to artificially generate air foam. The foam patch completely covered the 3 m x 7 m pool. The air flux can be regulated, with a maximum of 500 m^3 per hour.

V.2.1.2 Rain generator

One of the main goals of the FROG field experiment was to quantify the T_B variations at L-band due to the rain falling over the water surface. To generate controlled rain, a matrix of 14 diffusers were distributed along 3 rows (6 m long, 1.5 m wide) and was mounted on a crane at a maximum height of 13 m above the water surface (Figure 5.1a), from where the water drops reached the terminal velocity before splashing in the water pool. Also, from this height, the diffuser spot diameter is about 1 m, and hence the rainfall completely covered the 3 m x 7 m pool (Figure 5.1b).

(a)  (b) 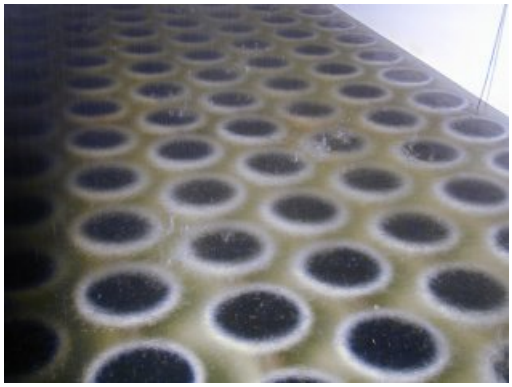

Figure 5.1. (a) Rain generator, and (b) water surface roughed by rain.

V.2.2 Instruments' description

During the FROG field experiment the required measurements were obtained from the following instrumentation:

- The LAURA L-band full-polarimetric radiometer (T_H, T_V, U, V) (UPC),
- A portable meteorological station (UPC), to measure the atmospheric pressure, temperature, relative humidity and rain rate,
- Two video cameras (UPC) to measure the foam coverage and the foam vertical profile,
- A water roughness meter (UPC) to measure the surface's height temporal evolution due to rain,
- A water conductivity meter (UPC) to determine the air-sea fraction beneath the foam layer,
- An infrared radiometer (UV) to provide SST estimates, and to measure the foam emissivity at IR frequencies,

- 6 temperature sensors (UV) located just below the water surface,
- A salinometer (IRTA), and
- The water samples acquired at each sequence, to be analyzed by the (ICM).

V.2.2.1 LAURA (L-band AUtomatic RAdiometer)

It is the main instrument of the FROG field experiment, and the same are used in the WISE field experiments. See chapter II for further details.

V.2.2.2 Video cameras

A video camera (model SONY SSC-DC393) with 752x582 pixels resolution, a 8.5 mm lens, auto-iris and 35.6°x25.2° field of view was mounted on the L-band radiometer pedestal as shown in Figure 5.2a. The analysis of the images restricted to a 20° field of view (coincident with the radiometer antenna beamwidth) have been used to:

- Evaluate the water surface foam coverage artificially generated by pumping air through a net of 104 air diffusers, Figure 5.2b by analyzing the image histograms,
- Estimate the sea foam emissivity by comparing the instantaneous sea foam coverage and the instantaneous brightness temperature (T_H and T_V).

(a)  (b) 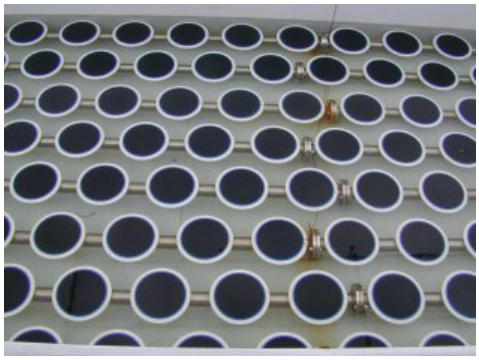

Figure 5.2. (a) Foam coverage video camera, and (b) array of air diffusers to create foam.

A second video camera (model Ultrak KC550xCP) with 512x582 pixels resolution and 5-50 mm lens, auto-iris and 5.4°x 4.1° field of view was mounted on a periscope along the rail, as shown in Figure 5.3a to take foam vertical profile images - reflected on a mirror tilted 45° to study:

- Bubbles' radii and their distribution and,
- The foam thickness layer,

in a wide range of salinities (foam fresh water to salt water, 38 psu) for a better understanding of the theoretical models (Figure 5.3b, and Figure 5.3c).

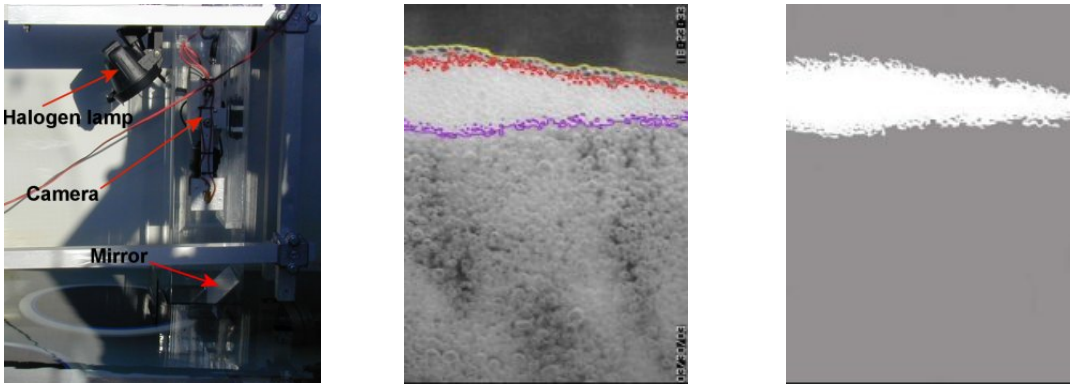

(a) (b) (c)

Figure 5.3. (a) Ultrak video camera inside of a periscope to acquire foam vertical profile images, (b) foam vertical profile acquired during FROG 2003 field experiment, and (c) separation of the foam layer.

V.2.2.3 Water roughness and air-fraction meter

The depth of two metal bars inside the water can be measured, since it is proportional to the conductivity measured between two metal bars, Figure 5.4a fed in AC, to avoid water electrolysis.

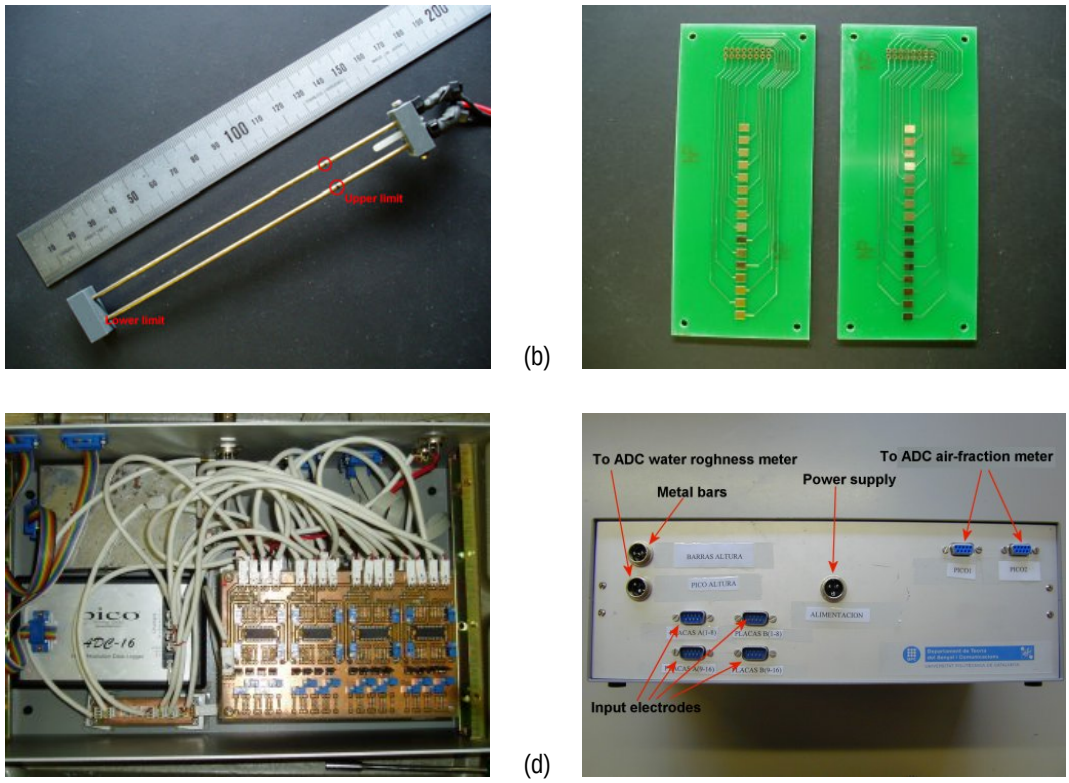

(a) (b) (c) (d)

Figure 5.4. (a) Brass bars used to measure the water surface roughness, (b) array of golden electrodes to obtain the air-water fraction content, water surface roughness and conductivity meter unit, (c) top view, and (d) front view.

Based on this principle, a water depth meter was designed and mounted to measure the water surface roughness induced by rain. As it will be seen in the next chapter, T_B numerical models strongly depend on the air-water fraction beneath the foam layer (f_a). A water conductivity meter was designed and mounted by UPC for this specific application. The instrument is composed by two parallel arrays of golden

electrodes (Figure 5.4b) separated 5 mm. Each electrode array is composed by an array of 16 patches (3 mm x 4 mm) separated 2 mm one from the other. A lacquer film protects the metallic tracks and the connector from the salt water. The foam conductivity is measured at all 16 pairs of electrodes simultaneously, from which the air-water fraction content can be estimated [17]. In Figure 5.4c and Figure 5.4d, the top and front views of the water roughness and air-fraction meter are shown.

Figure 5.5a and Figure 5.5b, the water roughness and air-fraction meter circuits schematics are shown. The Exar XR-2206 monolithic function generator generates a 1KHz sinusoidal wave with high temperature stability (20 ppm/°C) and low distortion (0.5%). Residual DC is cancelled by means of a potentiometer. The TS924 operational amplifier (O.A.), with high output current (80 mA) provides a voltage that it is proportional to the conductivity between the two metal bars, and hence proportional to the fraction of water, which covers the metallic bars. The AD536A is a monolithic integrated circuit that performs true rms-to-dc conversion to attack the ADC from *Picolog* (ADC-12). The ADC-12 is composed by one channel connected to the RS232 port, with a maximum signal level of 5V, and sampling frequency of 12 KHz. The sampling frequency is fixed to 200 Hz, to be able to sample high enough the maximum rainfall frequency [47]. The required signal conditioning circuitry is also implemented, as in the radiometer's ADC.

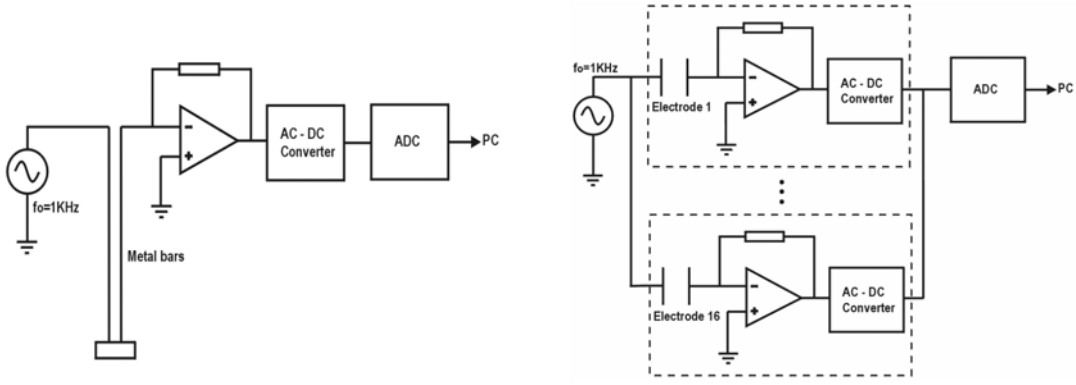

(a) (b)

Figure 5.5. Circuits schematic: (a) water roughness and, (b) air-water fraction meter.

The schematic of the air-water fraction and water roughness circuits are essentially the same. The air-water fraction circuit consists of the repetition of the water roughness circuit 16 times, one for each electrode and the sine wave generator output is buffered to attack the 16 TS924 O.A simultaneously. The conductivity of the n^{th} electrode depends on the air-water fraction of this specific electrode. Every rms output is converted to DC using the AD536A, and then connected to two high resolution (16 bits + sign) ADCs from *Picolog*.

V.2.2.4 Other instruments

A meteorological station from UPC (see chapter II) provided rain rate, atmospheric pressure, relative humidity, and air temperature at 3 m height. This meteorological station was connected to the

same computer as the radiometer (see previous section). The meteorological data were tagged with the GPS time and saved in the same files that the Stokes elements vector.

An infrared radiometer from the University of València (UV), model CIMEL CE 312 thermal-infrared radiometer to provide water surface temperature estimates including the presence of foam (see chapter III for more details).

(a) (b)

Figure 5.6. (a) temperature sensor, and (b) datalogger temperature sensor.

Six PT100 temperature sensors with a 0.1° C precision were distributed just below the sea surface (Figure 5.6a). The temperature data logger is shown in Figure 5.6b. As the memory size of data logger is 64 KBytes, approximately each 20 hours the data must be dumped to the laptop.

Measurements were acquired in a wide range of salinities, from 0 psu to 37 psu, by mixing salt sea water from the Mediterranean, and fresh river water from the Ebro. The water salinity of each experiment was first roughly estimated with a salinometer from IRTA (1-2 psu precision) and afterwards measured very accurately (0.001 psu) at ICM from the water samples acquired.

V.2.3 Summary of measurements and data products

Instrument	Parameters	Description	Units	Comments	Resolution
L-band pol-radiometer	T_H	Horizontal T_B	[K]	3-4 min (integration time)	< 0.3 K @ 1s
	T_V	Vertical T_B	[K]		< 0.3 K @ 1s
	U	Third Stakes Parameter	[K]		< 0.424 K @ 1s
	V	Fourth Stakes Parameter	[K]		< 0.424 K @ 1s
Clinometer	Pitch	Antenna orientation (±80°)	[deg]	Correct variation due to the strong wind	< 0.01°
GPS	Time	Absolute GPS time	[s]	Tag all measurements for easier comparison	1 sec
Motors		Antenna's elevation movement		Gear reduction included (1:750)	0.0006 °
		Antenna's azimuth movement		Gear reduction included (1:75)	0.006 °
Meteorological station	WS	Wind Speed	[m/s]	WS used only for safety purposes of the antenna	0.44 m/s
	WD	Wind Direction	[°]		1°
	RH	Relative Humidity	[%]		1%
	RR	Rain Rate	[mm/h]		0.25 mm/h
	P	Atmospheric Pressure	[mbar]		1 mbar
	T	Atmospheric Temperature	[°C]		0.05 °C
Infrared radiometer	IR data	IR camera on antenna (UV)	[K]	Estimate SST for cross-check with satellite and ground truth data (1 s integration time)	0.05 K (sensitivity)
Video camera	Video images	Video camera on antenna		To determine the water surface foam coverage	
	Video images	Video camera on a periscope		To analyze foam statistics	radii bubbles > 0.1 mm
Water roughness	Roughness	Surface roughness measure	[mm]	Inter comparison with the rain spectrum model	< 100 μm
Air-fraction meter	f_a	Air-water ratio	[%]	Apply it to the theoretical model	V_{ADC} = 0.3 mV
Conductivity meter	SSS	Sea Surface Salinity, estimate IRTA	[psu]	Estimate the salinity concentration	1 psu

V.2.4 Organization and logistic

V.2.4.1 Introduction

The FROG experiment is divided in three main tasks presented in Figure 5.7. The schedule of the project is presented in Figure 5.8.

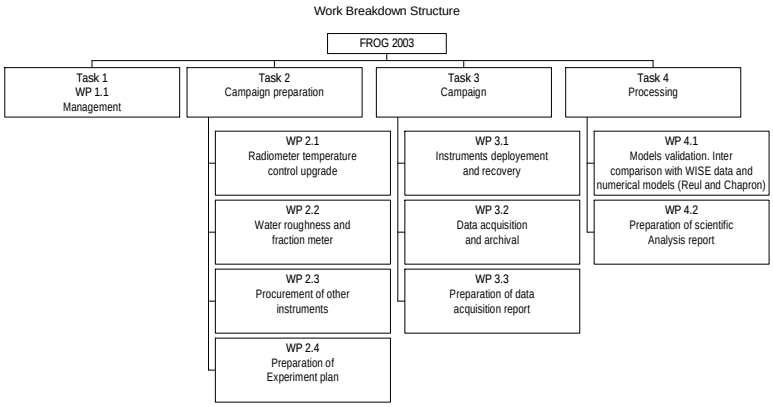

Figure 5.7. FROG breakdown structure

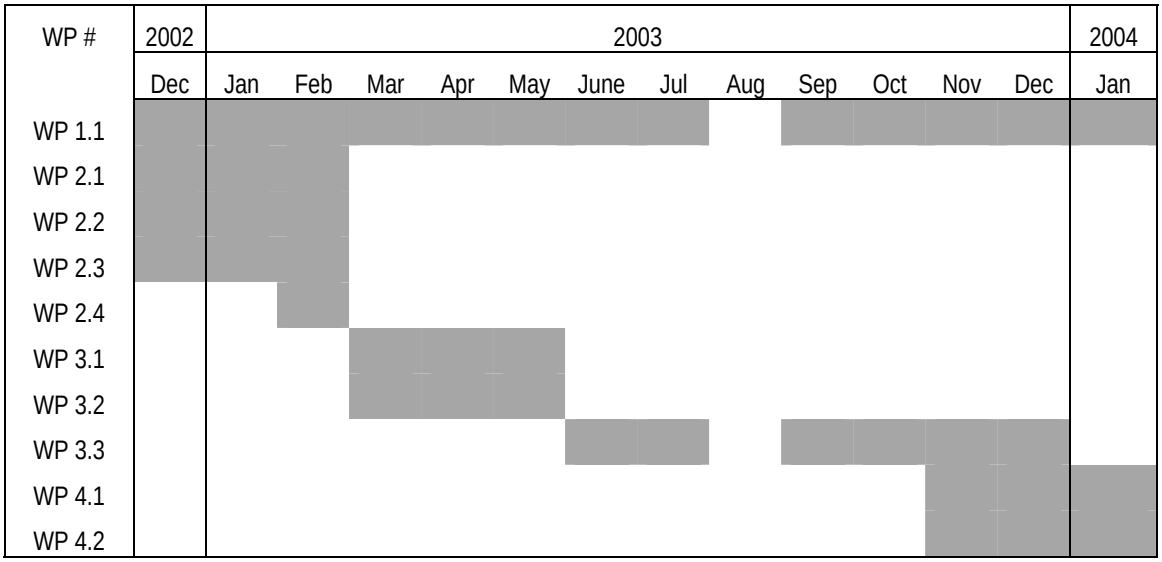

Figure 5.8. FROG 2003 scheduling

Basic dates of the campaign were: the FROG field experiment, that took place at the IRTA facilities from March 13th to May 5th, the first preliminary results were presented at the International Geoscience and Remote Sensing Symposium IGARSS 2003, held from July 21st to 25th, 2003 in Toulouse, and in the SPIE's 10 International Symposium of Remote Sensing, held from September 8th to 12th, in Barcelona. FROG results were presented at the 8th specialist meeting on Microwave Radiometry and Remote Sensing Applications, held from February 24th to 27th, in Rome.

WP 2.1, WP 2.2 and WP 2.3 are related to the instrument upgrade and are explained in chapters II and V. WP 2.3 is described in this chapter, and includes: the construction of the rain generator, the foam generator, and the periscope. Tasks 3 and 4 are explained in chapters V and VI.

V.2.4.2 Material preparation, transportation, and instruments deployment

The weeks previous to the beginning of the FROG field experiment were devoted to the campaign preparation. The IRTA facilities (Figure 5.9a) are located 40° 37' 33" N, 0° 37' 56" E in the South of Catalonia, in the Ebro River Delta (Figure 5.9b). The pool (Figure 5.9c) and the radiometer were placed in the position indicated in the plane shown in Figure 5.9d.

(a)

(b)

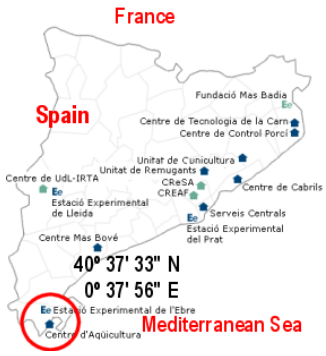

(c)

(d)

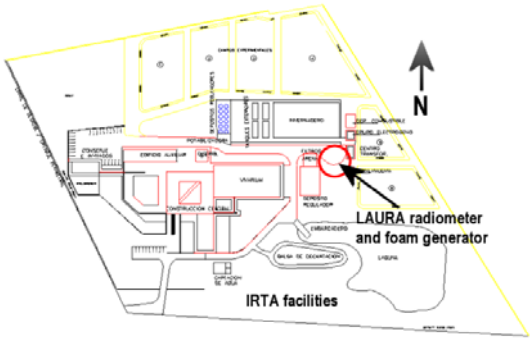

(e)

(f)

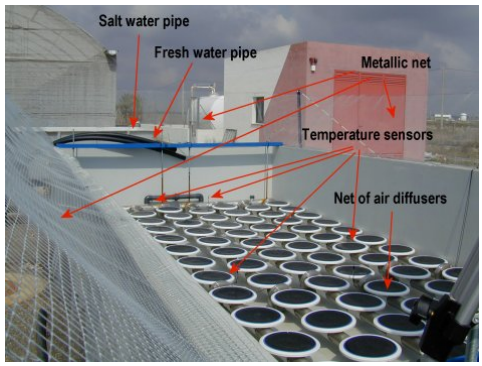

Figure 5.9. (a) IRTA facilities, (b) IRTA situation, (c) pool, (d) IRTA facilities plane, (e) container room, and (f) visual description of the set-up.

The control unit (CU) was mounted inside the container room (Figure 5.9e) to preserve the equipments from the hard environment conditions specially the salty humidity due to the proximity to the

coast. In Figure 5.9f, a picture of the set-up is shown. The multiple ranges of salinities are achieved, mixing the salt and fresh water.

The L-band radiometer was mounted pointing to the North, on a 1.5 m high pedestal (Figure 5.10). The radiometer was tightened with steel wires to improve its stability in case of strong winds (up to 140 Km/h), not uncommon in the area. The hot load was located behind the radiometer tied to a pile of bricks. The infrared radiometer was mounted on a tripod, and it was manually controlled.

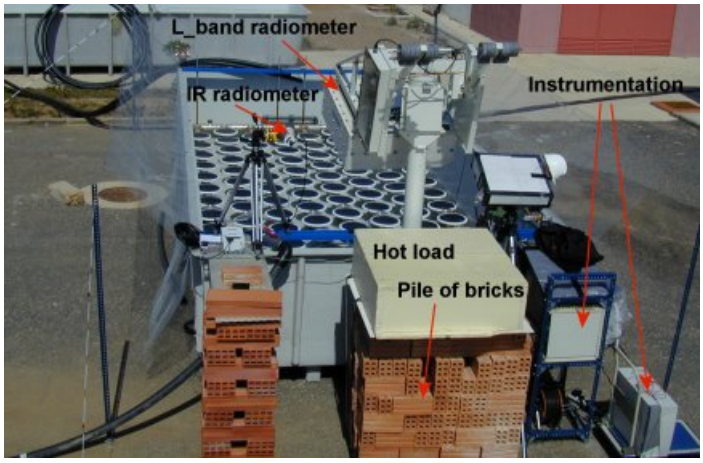

Figure 5.10. Picture of the instruments deployment.

The required power consumption was divided into the next parts:

- Electronic equipments: power radiometer, synthesizer, power computers, motor controllers, UPS, video cameras (~ 2 kW), (220 V, 50 Hz single phase),
- Peltier cells and fans, halogen lights and heater (~4.5 kW, 220 V, 50 Hz single phase),
- Pumping air generator, (~3.5 kW, 380 V, 50 Hz, three phases).

Total power consumption (~10 kW).

Another considerations to take into account were:

- The water flux to fill the pool was ~25 m^3/hour (Figure 5.9f and Figure 5.11a),
- A short right angle polyethylene tube (length = 50 cm, diameter = 90 mm) was connected to the pool draining hole with the opposite side open. The tube was in vertical position when the tank is filled and it was rotated 90° to empty the pool. The open side was connected to a plastic hose, flowing the water into the sea,
- The pumping air generator was connected to the array of air diffusers. Its flow was (~500 m^3/hour). The air flux was regulated through the air stopcock (Figure 5.11b). Different foam concentrations and thickness were achieved regulating the air stopcock. In this case, an air escape was mounted (Figure 5.11c) to avoid damages to the air pump,

- The rain generator was connected to an hydrant, to achieve enough water pressure and flux to generate an artificial rain rate of ~ 4,000 mm/h over 21 m^2 at 13 m high. During the rain experiment the pool was filled with fresh to avoid salinity variations,
- The metallic net assembly was divided into two parts: surrounding the pool and at 45° slope over the pool edges so as to enlarge the electric horizon (Figure 5.9f),
- A pair of halogen lamps were connected to take the video snapshots during the measurement acquisition.

(a)  (b)  (c) 

Figure 5.11. (a) Water stopcock, (b) air circuit and its air stopcock, and (c) air escape tube and its air stopcock.

V.2.4.3 Organization. Operators scheduling. Problems encountered

Four persons composed the team during the first ten days, (3 persons from UPC, and 1 person from UV). Support from specialized technicians from IRTA was provided. Among the main problems that had to be taken into account: the metallic net assembly and the hydrant for the rain measurements were probably the two more important.

The air diffuser array was covered with ~ 5 cm of water, to generate an acceptable foam volume, (see the circle in Figure 5.9f). To achieve the wide range of salinities between (0 psu to 34 psu), fresh and salt water were mixed following a trial and error empirical method. Table 5.1 summarizes the approximated mixing times required to achieve the specified salinity:

Table 5.1. Times in which the salt and fresh pipes have to be open, to achieve the required SSS

SSS (psu)	0	5	10	15	20	25	30	34
Salt water	00' 00"	02' 00"	04' 06"	06' 10"	08' 15"	10' 20"	12' 22"	14' 00"
Fresh water	14' 00"	12' 00"	09' 54"	07' 50"	05' 45"	03' 40"	01' 38"	00' 00"

At the end of each measurement, a water sample was taken and to be analyzed to determine the salinity concentration with a Guildline Autosal salinometer (resolution better than 0.001 psu).

After the initial period, the team was composed, most of the time by two persons during the period of measurements (approximately 40 days). Before the measurements were acquired, all the equipments

were synchronized to the GPS time, the pool cleaned, and filled with salt water with a specific salinity concentration according to Table 5.1. Measurements started after sunset to avoid any sun glint contamination.

Five types of measurements were undertaken:

- Foam measurements (total of 48 measurements) were divided in: 3 repetitions, of 8 salinities, and 2 different airflows to generate more or less foam. Each measurement consisted of 8 incidence angles, (from 20° to 55°, in steps of 5°). As differential measurements were acquired (3' no foam, 4' foam, and finally 3' no foam), one person had to go out to open/close the air stopcock, while the incidence angle movements were performed in an automatic manner. Foam, radiometric and infrared measurements were acquired separately. Foam measurements usually finished at 2:00 AM.
- Flat water measurements (a total of 21 measurements) were divided in: 3 repetitions, of 7 salinities (5 psu to 34 psu). Each measurement consisted of 36 incidence angles (20° to 55°, steps of 1°). Measurements were taken by automatic manner every 3'. Flat water measurements started at 2:00 AM and finished at 4:30 AM.
- Hot load and cold load measurements (total of 12 measurements) that consisted of pointing the radiometer first to the sky and then to the absorber during two hours at each position. The purposes of these measurements consisted of the acquisition of raw data to program the neural network, to improve even further the thermal stability control, and second to estimate the radiometer sensitivity of the two channels. Measurements were taken of automatic manner from 4:30 AM to 8:30 AM.
- Rain measurements (1 measurement), were performed with fresh water to avoid salinity variations and at 8 incidences angles (from 20° to 55°, in steps of 5°). For these measurements the participation of three persons was required. Differential measurements were also acquired in three steps (2' no rain, 2' rain, and 2' no rain), one person opened and closed the stopcock. During the third step, the radiometric data was acquired, but not processed, since the water pipes were still leaking water. Simultaneously, conductivity measurements of the water surface roughness were acquired. Although the planned rain measurements were 6 scans, it was not possible to perform them because the fire water pump crashed twice. On the other hand, maximum height of the elevator crane was fixed to 13 m, high enough to guarantee that the water drops reach their terminal velocity.
- Oil slicks measurements (total of 4 measurements). T_B was measured at 8 incidence angles from 20 ° to 55° for fresh water a salt water (34 psu), being the amount of oil 0.5 liters and 1 liter. These measurements were acquired at the end of the field experiment due to the difficulty of cleaning the oil slicks. Even though these were thick oil slicks as compared to the

ones found in the sea at L-band, and according to the theoretical model, much more than 1 liter of oil would be needed to observe a detectable brightness increase, (see chapter VI).

V.3 Radiometric measurement strategy

V.3.1 Previous considerations to the radiometric measurements

Although the radiometric sensitivity to SSS at L-band is almost maximum, even at this frequency it is low: 0.5 K per psu at 20 °C. LAURA's sensitivity at 1 s integration time is close to this value. For this reason a larger integration time (~1 min) is required to improve the radiometric sensitivity below this value. On the other hand, the maximum integration time depends on the stationary properties of the water conditions.

Another effect to consider is the galactic noise. If the galactic center is not imaged, its contribution is relatively constant over long periods of time. However, its time-dependence is modeled using the measured radiometer antenna pattern and the 1,420 MHz brightness temperature maps [18] and [48]. To minimize this contribution the radiometer was pointed to the North.

Sun glitter can seriously perturb the radiometric measurements. To avoid completely this effect all measurements were acquired during nighttime.

V.3.2 Type of radiometric measurements

Two types of measurements were performed:

- Calibration: at the beginning and at the end of each measurement cycle (limited to less than 100 min).
    - ♦ Calibration of the Dicke radiometers is performed by looking to the sky (cold source) and to a microwave absorber at known ambient temperature (hot load). An elevation angle of 145° (35° from zenith) pointing to the North was used for the sky view. Atmospheric effects are estimated from numerical models (atmospheric pressure, temperature and relative humidity) assuming a horizontally stratified atmosphere. The effect of galactic noise is taken into account from the antenna position and orientation, the date and time, the antenna pattern and the map of galactic noise at 1,420 MHz [18] and [48].
    - ♦ Calibration of correlator's offsets is performed by injecting uncorrelated noise (independent matched loads), while phase is calibrated by injecting known and common correlated noise. In both cases the radiometer's antenna is disconnected. This process is performed automatically, even though the data corresponding to the third and fourth Stokes parameters has not been analyzed.

- Incidence angle measurements: to determine the variation of the T_H and T_V with the incidence angle. The following angles have been measured: 20°, 25º, 30°, 35º, 40°, 45º, 50° and 55º. This was the normal mode of operation. All these measurements were repeated in a wide range of salinities from ~0 psu to ~34 psu in ~5 psu steps.

In Figure 5.12a and Figure 5.12b, two pictures of the radiometer pointing to the hot load calibration and pointing to the swimming pool $\theta = 45°$ are shown.

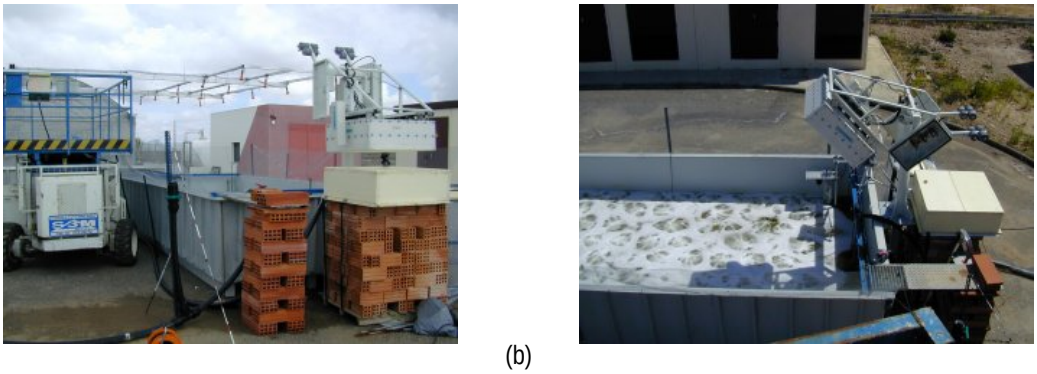

(a) (b)

Figure 5.12. (a) Radiometer pointing to the hot load, and (b) pointing to the foaming pool.

V.3.3 Foam contribution to T_B

The strategy of the foam measurements consisted of measuring the T_B at horizontal and vertical polarizations at 8 incidence angles and for 8 different salinities. The total measurement time at each position was 10 minutes (3 minutes measuring T_B without foam, 4 minutes measuring T_B with foam, 3 minutes measuring T_B without foam again). The foam-induced brightness temperature ($\Delta_F T_B$) is clearer seen using these differential measurements. The diffuser's air flux was controlled to get different foam coverage percentages, and thickness.

V.3.3.1 Foam surface's cover acquisition

To determine the impact of foam in the T_B, the SONY video camera was mounted pointing to the radiometer's FOV. Since each image pixel corresponds to a different distance and incidence angle, their area must be first determined [49]. The determination of the foam-covered pixels consists of computing the image histogram as in WISE field up (chapter IV), and selecting the pixels with grey levels higher than a given threshold [49].

(a) 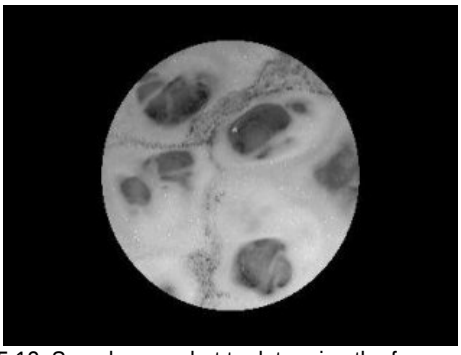 (b) 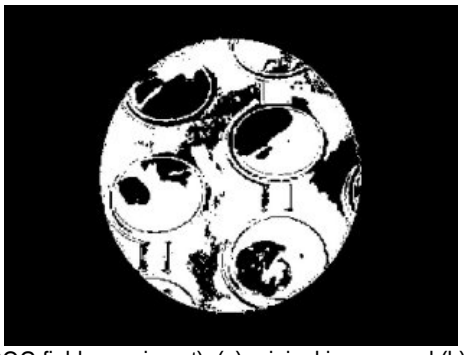

Figure 5.13. Sample snapshot to determine the foam coverage (FROG field experiment), (a) original image, and (b) processed image (foam fraction in half-power spot: 69.8 %).

Assuming that the generated foam in the FROG field experiment presented stationary properties, the frame rate was about 1 frame every 10 seconds. The total number of frames per position analyzed was about 25. In Figure 5.13a one of the images acquired during FROG experiment is shown, (radiometer was pointing at θ = 35°), and in Figure 5.13b its binaryzed, (b/w levels) image. For this case, the computed foam coverage percentage is 69.8%.

V.3.3.2 Foam vertical profile acquisition

The main goal of this additional measurement consisted of determining several of the parameters of the theoretical models: the average bubbles radius (r_p), the determination of different foam layers, and the foam layer thickness, d. The frame rate was about 3 frames per second.

V.3.3.3 Determination of the void fraction beneath the foam layer

Another parameter that contributes to the T_B theoretical model is the air-water fraction beneath the foam layer. For this, a water conductivity meter was used over the whole range of salinities. From Figure 5.14a to Figure 5.14e the conductivity meter experiment is shown. Foam was generated by an air-compressor connected to one diffuser. The instrument calibration consisted of making two steps: a) placing the instrument completely inside the calm water and, adjusting the signal amplification from each electrode, by means 16 potentiometers to achieve the same output voltage in every electrode, and b) measuring the residual output voltage of each electrode without water, that will be subtracted from the measurements.

The relative conductivity can be expressed (eqn. (5.1)) as the relationship between the output voltage of each electrode, when the foam is generated, and the output voltage of every electrode placed inside the water, and calibrated according to steps (a) and (b),[17].

$$\sigma = \frac{\left(\sigma_{foam} - \sigma_{air}\right)}{\left(\sigma_{water} - \sigma_{air}\right)}, \tag{5.1}$$

on the other hand, Curtayne's eqn. relates the liquid fraction(ϕ_l) and the foam/water conductivity (σ), as :

$$\sigma = \frac{1}{3}\left(\phi_l + \phi_l^{1.5} + \phi_l^2\right), \tag{5.2}$$

from which, the void fraction beneath the foam layer f_a can written as (eqn. (5.3)):

$$f_a = 100 \cdot \left(1 - \phi_l\right). \tag{5.3}$$

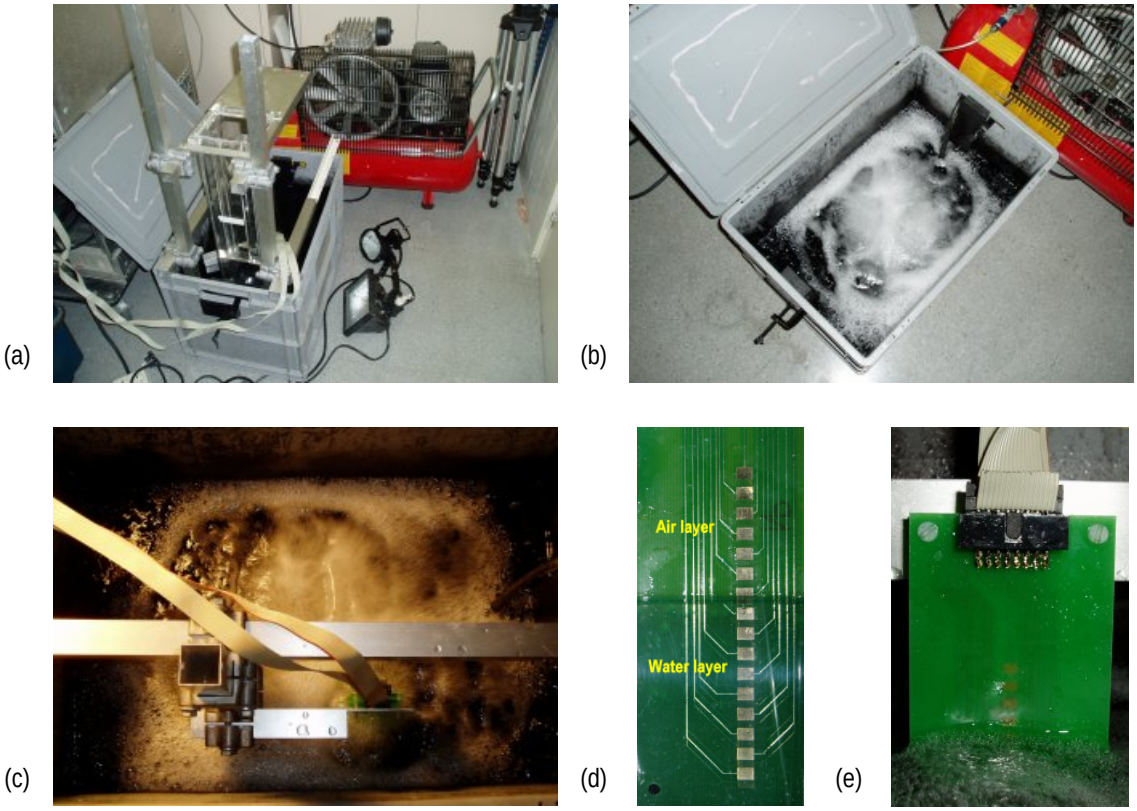

Figure 5.14. Void fraction beneath the foam layer measurement, (a), (b) experimental set-up, (c) to (e): conductivity meter.

V.3.4 Influence of the rain and water surface roughness

V.3.4.1 Rain-perturbed radiometric measurements

To determine the impact of rain in T_B, a rain generator was mounted at 13 m height (Figure 5.15a). At 1.4 GHz the attenuation due to rain is known to be low, but the impact of the rain in the surface roughness and the associated emissivity increase was unknown. The purpose of this measurement is to quantify the rain-induced ΔT_B. The strategy consisted of measuring T_B at the horizontal and vertical polarizations, at the 8 incidence angles (20° to 55° in 5° steps), with and without rain. The total time at each measurement position was 6 minutes (2 minutes measuring T_B without rain, 2 minutes measuring T_B with rain, and 2 minutes measuring T_B without rain again). Differential measurements were performed as

in the foam measurements case to increase the accuracy. The water source pressure was 8 kg per cm^2 to feed the net of shower diffusers, and the equivalent rain rate was approximately 4000 mm/h.

V.3.4.2 Rain-perturbed water surface roughness measurement

In order to compare the observed ΔT_B with sea surface emissivity models with precipitation, as well as to determine the quantity of rain that had fallen, the water roughness measuring system from UPC was used. As described in chapter II, the instrument is based on a conductivity measurement. Due to the high variability of the surface height (<100 Hz), the output signal is sampled with an ADC12 data logger at a 200 Hz frequency rate. Water surface's height roughness and, rain radiometric measurements were performed simultaneously.

The process is divided in two steps. First of all the calibration of the metal bars is made, which is performed by placing the bars inside the water, in the upper and in the lower limits, and taking samples with the ADC converter. The surface's height is then proportional to the voltage variation between these two positions. Roughness data are acquired after the calibration process.

Figure 5.15. Rain generator mounted at 13 m.

V.3.5 Oil slicks radiometric measurements

Another parameter that contributes to the T_B measurements over the ocean is the presence of oil slicks. A total of four measurements of T_B were made, by mixing fresh and salt water with 0.5 l and 1 l of mineral oil, following the incidence scans sequence. A small number of measurements were only made because of the difficulty to clean the pool, and to eliminate the residual oil. Furthermore oil slicks measurements were made during the last days of the campaign to keep clean the air pump diffusers.